

Climate of the Past Discussions is the access reviewed discussion forum of *Climate of the Past*

Changes in
atmospheric
variability in a glacial
climate

F. S. R. Pausata et al.

Changes in atmospheric variability in a glacial climate and the impacts on proxy data: a model intercomparison

F. S. R. Pausata^{1,2}, C. Li^{1,3}, J. J. Wettstein¹, K. H. Nisancioglu¹, and
D. S. Battisti^{2,4}

¹Bjerknes Centre for Climate Research, Allegaten 55, 5007 Bergen, Norway

²Geophysical Institute, University of Bergen, Allegaten 70, 5007 Bergen, Norway

³Department of Earth Science, University of Bergen, Allegaten 41, 5007 Bergen, Norway

⁴Department Atmospheric Sciences, University of Washington, Seattle, WA 98195, USA

Received: 11 February 2009 – Accepted: 11 February 2009 – Published: 12 March 2009

Correspondence to: F. S. R. Pausata (francesco.pausata@bjerknes.uib.no)

Published by Copernicus Publications on behalf of the European Geosciences Union.

Title Page

Abstract

Introduction

Conclusions

References

Tables

Figures

⏪

⏩

◀

▶

Back

Close

Full Screen / Esc

Printer-friendly Version

Interactive Discussion

Abstract

We investigate sea level pressure variability in the extratropical North Atlantic in the preindustrial climate (1750 A.D.) and at the Last Glacial Maximum (LGM, 21 kyr before present) using four climate models. In general, the models exhibit a significant reduction in interannual variance of sea level pressure during the LGM compared to pre-industrial simulations and this reduction is concentrated in winter.

For the preindustrial climate, all the models feature a similar leading mode (EOF) of sea level pressure variability that is also similar to the leading mode of variability in the instrumental record: the North Atlantic Oscillation (NAO). In contrast, the leading mode of sea level pressure variability during the LGM is model dependent, but in each model different from that in the preindustrial climate. In each model, the leading (NAO-like) mode of variability explains a smaller fraction of the variance and also less absolute variance in the LGM than in the preindustrial. The leading (NAO-like) mode of sea level pressure variability is shifted southward in the LGM simulations relative to the preindustrial simulations.

Finally, we correlate the leading mode of sea level pressure variability with surface temperature and precipitation within each model and for the two time periods. In the preindustrial climate, the leading mode of sea level pressure variability is similar from model to model and the temperature and precipitation correlation patterns are also similar. In contrast, since the models find different dominant modes of sea level pressure variability for the LGM climate, they also disagree on the associated patterns of temperature and precipitation variability. Assuming stationarity of the relationship between surface climate and the leading mode of sea level pressure variability could lead to a misinterpretation of signals recorded in proxy data.

CPD

5, 911–936, 2009

Changes in atmospheric variability in a glacial climate

F. S. R. Pausata et al.

Title Page

Abstract

Introduction

Conclusions

References

Tables

Figures

⏪

⏩

◀

▶

Back

Close

Full Screen / Esc

Printer-friendly Version

Interactive Discussion

1 Introduction

Northern Hemisphere climate variability is dominated by patterns of variability including the North Atlantic Oscillation (NAO: Hurrell, 1995) or the closely related Northern Annular Mode (NAM: Thompson and Wallace, 2000). The fact that observed NAO indices exhibit low-frequency variability (e.g. Luo et al., 2007) has led to interest in how the mode may be influenced by both past and future climate changes, when the atmosphere experienced large perturbations in greenhouse gases and land ice extent relative to today. Attempts to reconstruct the NAO index over the past few hundreds years have been made using proxies, which record variations in either temperature or precipitation (e.g. Barlow et al., 1993; Appenzeller et al., 1998a,b). For instance, in the present climate the NAO index is strongly negatively correlated with snow accumulation on the western Greenland Ice Sheet (Appenzeller et al., 1998a; Hutterli et al., 2005). However, various pre-instrumental NAO reconstructions do not show significant agreement (Luterbacher et al., 2002). It has been suggested that changes in the position of the centers of action of the NAO have led to a change in the signal recorded by the proxies (Christoph et al., 2000; Raible et al., 2006).

Climate models can help to assess how internal atmospheric variability may be altered by external forcings, and how these changes may affect the signal recorded in proxy data. For example, model simulations suggest that persistent positive anomalies in the NAO index in the 1980–1990s are linked to increases in greenhouse gas concentrations (Shindell et al., 1999; Miller et al., 2006). Past climates offer a wider range of climate states to explore, in addition to the possibility of comparing model simulations with proxy observations when and where these are available. Previous studies have shown that during the mid-Holocene (MH; 6000 yr before present or 6 ka) warm interval, the atmosphere supports variability that has NAO-like characteristics similar to the pre-industrial (PI, 1750 A.D.) period (Gladstone et al., 2005). On the other hand, simulations of the Last Glacial Maximum (LGM, 21 ka) cold climate exhibit substantial differences in both the mean state and variability of the extratropical circulation com-

CPD

5, 911–936, 2009

Changes in atmospheric variability in a glacial climate

F. S. R. Pausata et al.

Title Page

Abstract

Introduction

Conclusions

References

Tables

Figures

⏪

⏩

◀

▶

Back

Close

Full Screen / Esc

Printer-friendly Version

Interactive Discussion

pared to PI simulations. These differences include:

1. a southward shift of the Pacific and Atlantic storm tracks (Lainé et al., 2008);
2. a shift (Justino and Peltier, 2005; Peltier and Solheim, 2002) and weakening (Otto-Bliesner et al., 2006) of the NAO's main centers of action; and
3. a decrease in interannual jet variability and storminess in the Atlantic sector (Li and Battisti, 2008).

However, it is difficult to evaluate how robust the changes in atmospheric variability are and how the relationship between changes in the atmospheric flow patterns and proxy signals varies, because each of the aforementioned studies (with the exception of Lainé et al., 2008) was performed using a single model.

We present a model intercomparison of atmospheric variability in the extratropical Northern Hemispheric (20° – 90° N) as represented by sea level pressure (SLP) in two fundamentally different climate states, the PI and the LGM. The LGM simulations permit an exploration of the dominant patterns and seasonality of climate variability during an interval when the atmospheric circulation was substantially perturbed by the presence of large land-based ice sheets and by lower greenhouse gas concentrations. The LGM simulations also give us the possibility of investigating whether or not the variability recorded in proxy data is representative of the variability over larger spatial scales. In general, the LGM simulations exhibit:

1. a significant reduction in interannual variance of extratropical SLP;
2. a decrease in the amount of total interannual variance captured by the leading (NAO) mode of variability;
3. a southward shift and a weakening of the centers of action associated with NAO variability;
4. a damping of the seasonal cycle of interannual variance of SLP;

Changes in atmospheric variability in a glacial climate

F. S. R. Pausata et al.

Title Page

Abstract

Introduction

Conclusions

References

Tables

Figures



Back

Close

Full Screen / Esc

Printer-friendly Version

Interactive Discussion



5. a modification of the leading patterns of spatial covariability in precipitation and surface temperature.

This work is structured as follows: Sect. 2 gives a description of the coupled models used and the boundary conditions for the PI and LGM climates; Sect. 3 presents the changes in the spatial pattern of SLP variability in the Northern Hemisphere (NH) and the distribution of this variability over the seasonal cycle; Sect. 4 discusses the paleoclimate implications of changes in the mean circulation and its variability in the signal recorded in proxies; conclusions are presented in Sect. 5.

2 Model data sets

The model output analyzed belongs to the Paleoclimate Modelling Intercomparison Project Phase II (PMIP2, <http://pmip2.lsce.ipsl.fr>). The subset of PMIP2 models used in this study includes: the Community Climate System Model 3.0 (CCSM3), the Institut Pierre-Simon Laplace model (IPSL), the Hadley Centre Coupled Model version 3 (HadCM3M2) and the Model for Interdisciplinary Research on Climate version 3.2 (MIROC3.2). The horizontal resolution in the atmosphere varies slightly between models, but has a nominal grid spacing of 300 km or T42 in a spectral model. Boundary conditions for the two climate states (PI and LGM) follow the protocol established by PMIP2. In the PI simulations, the orbital configuration is set to 1950 A.D. values; the greenhouse gases correspond to 1750 A.D.; and vegetation is prescribed to a model-dependent present day distribution. In the LGM simulations, the ice sheets are prescribed according to the ICE-5G reconstruction (Peltier, 2004); the orbital configuration is set to 21 ka, which is similar to the modern values; the vegetation is the same as in the PI; and the concentrations of greenhouse gases are lower, resulting in a decrease in a tropospheric radiative forcing of approximately 2.8 W m^{-2} relative to the PI climate (Braconnot et al., 2007). For all the models, 100 years of monthly post-spinup SLP, temperature and precipitation data from 20° – 90° N are analyzed for both the LGM and PI simulations. The Atlantic sector is defined as 20° – 90° N, 120° W– 45° E using the

Changes in atmospheric variability in a glacial climate

F. S. R. Pausata et al.

Title Page

Abstract

Introduction

Conclusions

References

Tables

Figures

⏪

⏩

◀

▶

Back

Close

Full Screen / Esc

Printer-friendly Version

Interactive Discussion



Rocky Mountains and the Urals as boundaries; however, the results presented here are not sensitive to the exact definition of the sector.

3 Variability in the atmospheric circulation

This section is divided in three parts. The first two parts present, respectively the spatial patterns of SLP variability in the NH and the distribution of this variance over the seasonal cycle. The last part discusses some possible mechanisms behind the changes in variability of the atmospheric circulation. All differences discussed hereafter are significant at the 1% confidence level. The observed SLP variability (ERA40 reanalysis) is shown in Appendix A in a series of figures analogous to those presented in this section.

3.1 Spatial distribution of the SLP variance

In three out of four models, the interannual variability of NH SLP is reduced in the LGM simulations compared to the PI simulations (Fig. 1). The differences in standard deviation (σ) are largest in the high latitudes, especially along the east coast of Greenland, in the Northeastern Pacific Basin along the coast of Alaska, and over the Barents Sea (Fig. 1, right panels). Averaged over the extratropical NH, the model simulations exhibit a significant decrease in standard deviation of SLP in the LGM compared to the PI (Fig. 1), ranging from 6% in IPSL to 16% in HadCM3M2. Only MIROC3.2 shows a small and not significant increase from the PI to the LGM. A reduction in interannual variance is also observed in the free troposphere as seen in 500 hPa geopotential heights (not shown) and (Li and Battisti, 2008) documented a decrease in jet level wind variance in the CCSM3 simulation of the LGM.

The first EOF of monthly averaged SLP anomalies (after the seasonal cycle has been removed) in the North Atlantic sector demonstrates that an NAO-like feature is the dominant pattern of climate variability in the LGM simulations, though it represents less

Changes in atmospheric variability in a glacial climate

F. S. R. Pausata et al.

Title Page

Abstract

Introduction

Conclusions

References

Tables

Figures

⏪

⏩

◀

▶

Back

Close

Full Screen / Esc

Printer-friendly Version

Interactive Discussion

Changes in atmospheric variability in a glacial climate

F. S. R. Pausata et al.

Title Page

Abstract

Introduction

Conclusions

References

Tables

Figures

⏪

⏩

◀

▶

Back

Close

Full Screen / Esc

Printer-friendly Version

Interactive Discussion

total interannual variance than in the PI. The fraction of variance captured by the first LGM mode (λ_1) is reduced in all models (Fig. 2 and Table 1). Taking into account the reduction in total interannual variance averaged over the North Atlantic sector (σ_{NA}^2), these percentages reflect a decrease in standard deviation explained by the first mode ($\sqrt{\lambda_1 \sigma_{NA}^2}$) of up to 28% in CCSM3 (Fig. 2 and Table 1). These results are in qualitative agreement with the study of (Otto-Bliesner et al., 2006), which examined the NAO-like variability in the CCSM3 model.

In the LGM simulations, the NAO-like pattern is qualitatively similar to that in the PI. However, both the centers of action and the resultant pressure gradient of EOF1 are weaker in the LGM simulations, although they remain comparable to the PI EOF1 in two models (HadCM3M2, MIROC3.2). Though there is no agreement on the exact placement of the dominant lobes of variability among the models, each model shows a shift south/southeastward of the EOF1 pattern in the LGM relative to the PI. In two models the southern lobe moves southeastward towards the Mediterranean Sea, qualitatively similar to what was seen in the studies of (Justino and Peltier, 2005) and (Peltier and Solheim, 2002).

3.2 Seasonal cycle of variability

The general reduction in total interannual variance in the LGM simulations compared to the PI simulations is not evenly distributed across the year. Figure 3 shows the seasonal cycle of interannual standard deviation of SLP for all the model simulations. Reductions in interannual variability during the LGM are more prominent in winter, the season with the most interannual variability. In summer and early fall changes are smaller and often not statistically significant.

The dominant NAO-like variability (Fig. 2) also tends to exhibit reductions that are concentrated in winter (Fig. 4), suggestive of a dynamically consistent model response. The spread of the PC1s in a given month is an indication of the interannual variability in the leading mode for that month. The histogram spreads are narrower in the LGM

compared to the PI simulations, except in MIROC3.2 where the changes are significant only in winter.

In the LGM simulations, the amplitude of the seasonal cycle of total standard deviation is significantly reduced in all models compared to the PI simulation (Fig. 3, Table 1).

The reduced seasonal cycle of interannual standard deviation is also seen aloft (for example, in the analysis of 500 hPa geopotential heights, not shown). This suggests that the decrease of both interannual variability and the seasonal cycle of variability are dynamically driven.

3.3 Discussion

The LGM simulations show a significant reduction in interannual SLP variance and a weakening in the dominant pattern of variability relative to the PI simulations. The causes of these changes are poorly understood; however, they must be related to the remarkable differences in LGM climate compare to modern climate: a) presence of ice sheets over North America and Eurasia, b) reduced greenhouse gas concentrations, and c) changes in surface properties, such as sea ice and snow cover.

The large Laurentide ice sheet creates an upstream-blocking situation that may be related to a stronger but less variable subtropical jet stream in the Atlantic (not shown) during the LGM relative to PI. This change in jet stream variance is consistent with the reduction in the variance of the SLP field and of the leading EOF of SLP (the NAO) documented here. The decrease in flow variability during the LGM is also observed at the synoptic scale (Li and Battisti, 2008; Donohoe and Battisti, 2009).

Greenhouse gases and sea ice, both of which are applicable to future climate change scenarios as well as past climates, could also play a role in damping variability in the LGM simulations. Feldstein (2002) showed that the recent increase in NAO variance is in excess of what would be expected from internal atmospheric variability alone, thus implying that external factors such as the increase in greenhouse gas concentrations and/or changes in surface properties must be involved. Indeed, sea ice anomalies in the North Atlantic have been shown to affect the phase and amplitude of the NAO,

Changes in atmospheric variability in a glacial climate

F. S. R. Pausata et al.

Title Page

Abstract

Introduction

Conclusions

References

Tables

Figures

⏪

⏩

◀

▶

Back

Close

Full Screen / Esc

Printer-friendly Version

Interactive Discussion



producing large changes in sensible and latent heat fluxes that have feedbacks onto the atmospheric circulation (Deser et al., 2000; Gong et al., 2002; Seierstad and Bader, 2008). In addition, other factors such as changes in tropical sea surface temperatures could be relevant (Yin and Battisti, 2001).

5 4 Paleoclimate implications

Changes in the mean and variability of the atmospheric circulation, in the dominant modes of circulation variability, or in the seasonality of any of these components are interesting from a dynamical stand point, but they could also have a demonstrable effect on the signal recorded in climate proxies.

10 The statistical reconstruction of past climate from proxies is based on the idea that natural archives record variations in temperature, precipitation, or some combination of these and other factors. Reconstructions of surface climate variability over recent centuries have been performed using archives such as tree rings (e.g. Glueck and Stockton, 2001), pollen in lake sediments (e.g. Voigt et al., 2008) and ice cores (e.g. Appenzeller et al., 1998a). A common goal in selecting proxy records is to choose
15 sites where local variability is representative of larger (regional) scale variability. For example, in the present climate, surface temperature and precipitation in the Atlantic sector are coherently coupled with the NAO (e.g. Hurrell, 1995), such that any site able to capture NAO variability will also capture dynamically linked aspects of regional climate variability.
20

There have also been studies attempting to reconstruct climate variability patterns in different climate states (e.g. Bakke et al., 2005; Bahr et al., 2006). A particular challenge is that the same geographic site may record a qualitatively different mixture of mean and variance contributions in different climates. For example, the leading
25 mode of atmospheric circulation might change (see Sect. 3), resulting in a center of action shifting towards or away from the proxy site. If seasonality affects the proxy, a change in how variability is distributed throughout the year would affect the signal

Changes in atmospheric variability in a glacial climate

F. S. R. Pausata et al.

Title Page

Abstract

Introduction

Conclusions

References

Tables

Figures



Back

Close

Full Screen / Esc

Printer-friendly Version

Interactive Discussion



that the proxy records. The relative prominence of large scale variability in determining surface climate over a region might also change, implying that the proxy signal would reflect a different combination of changes in regional and local effects.

Here, we examine correlation statistics between surface temperature or precipitation and the leading mode of SLP variability in the model simulations. The goal is to compare the relationship between the leading mode and these other aspects of surface climate variability in the PI and LGM climate states. We present results from two of the four models, CCSM3 and HadCM3M2. These two models represent the most disparate responses in these correlation analyses; thus, they allow us to show the similarities in behaviour where all the models agree, and the range of behaviour where the models disagree.

In the PI simulations, interannual surface climate variability is coherently linked to patterns of the leading mode of SLP variability in all the models. First, we observe that the correlation of surface temperature (Fig. 5a,c) and precipitation (Fig. 6a,c) with the leading mode in the PI climate exhibits similar patterns in each model (Table 2). The high correlations with precipitation over western Greenland are consistent with the conclusions of (Appenzeller et al., 1998a), who used the data from a west Greenland ice core (NASA-U) and (Hutterli et al., 2005), who used snow accumulation from ERA40 reanalysis.

To assess whether the leading mode is able to describe the regional scale variability, we construct coherence maps for temperature and precipitation (Figs. 5 and 6 panels e and g). In these maps, high values indicate that the total variability at that location is strongly related to the total variability over the entire North Atlantic region. Note that maxima in the coherence maps are collocated with maxima in the correlation maps. This correspondence suggests that points where surface temperature and precipitation reflect leading mode variability are also points where the local variability does well in representing the larger scale variability in the PI climate, as is also the case in the present climate (Hurrell, 1995).

Similar analyses for the LGM simulations produce qualitatively different results. First,

Changes in atmospheric variability in a glacial climate

F. S. R. Pausata et al.

Title Page

Abstract

Introduction

Conclusions

References

Tables

Figures



Back

Close

Full Screen / Esc

Printer-friendly Version

Interactive Discussion

Changes in atmospheric variability in a glacial climate

F. S. R. Pausata et al.

Title Page

Abstract

Introduction

Conclusions

References

Tables

Figures

⏪

⏩

◀

▶

Back

Close

Full Screen / Esc

Printer-friendly Version

Interactive Discussion

the models do not agree on the pattern of surface temperature and precipitation associated with the leading mode of variability (Table 2). HadCM3M2 shows high correlations extending well into the subtropics (Figs. 5d and 6d), while CCSM shows correlations more confined to the northwest Atlantic sector (Figs. 5b and 6b). The other two models exhibit behaviour intermediate to these endmembers (not shown). And while the coherence and correlation maps correspond well for HadCM3M2, they do not for CCSM3. So there is considerable uncertainty regarding the relationship between surface climate variability and the leading mode of SLP variability in the LGM climate.

The results presented in this section collectively suggest that the link between leading modes of atmospheric and surface climate variability may well change over different climate states. Making an assumption that the link remains stationary could lead to a misinterpretation of proxy signals recorded over periods spanning large climate changes. For example, a proxy site could periodically be influenced by polar air masses in one climate, but not in another climate, even if the mean atmospheric circulation over the region were to change by very little. It is difficult to draw more concrete conclusions for the specific case of the LGM given that the models are not able to depict a consistent spatial pattern of surface climate variability in this climate state. However, in a few areas where the models do agree, it is possible to infer that a substantial amount of regional variability can be reliably reproduced in certain areas such as southern Norway or Labrador (Fig. 7, Table 3).

Reconstructing surface climate and NAO-like variability in the LGM climate is particularly complex, but the interaction of changes to the mean atmospheric circulation and to its variability could dramatically influence proxy records. Moreover, the dominant patterns of atmospheric variability themselves might change in intensity, location or relevance to surface climate variability.

5 Conclusions

In this paper, we analyze surface climate variability in the extratropical North Atlantic in simulations of LGM and PI climate from four climate models, and investigate how changes in this variability may affect signals recorded in proxy data. The main findings include the following:

- Interannual variability of Northern Hemisphere sea level pressure is significantly reduced in the LGM.
- The seasonal cycle of sea level pressure variance is decreased during the LGM. The reduction is more prominent and significant in the winter months, when the variability is highest.
- An NAO-like pattern is the dominant mode of interannual SLP variability in each LGM simulation examined, though it represents less total variance and the centers of action are weaker.
- The changes in the atmospheric variability lead to a southward shift of the pattern of correlation between temperature/precipitation and the NAO-like index in the LGM.
- The link between leading modes of atmospheric and surface climate variability may change over different climate states. In particular, surface temperature variability in the North Atlantic may not be dominated by NAO-like variability in the LGM, implying that proxy data of all sorts could be affected by non-stationarity.

Appendix A

In order to compare the results of the models in the PI simulations with modern observations, the same analyses have been performed using the ERA40 reanalysis data set and are shown in Fig. 8.

Changes in atmospheric variability in a glacial climate

F. S. R. Pausata et al.

Title Page

Abstract

Introduction

Conclusions

References

Tables

Figures



Back

Close

Full Screen / Esc

Printer-friendly Version

Interactive Discussion



Acknowledgements. The present work is part of the ARCTREC project and funded by the Norwegian Research Council. We acknowledge the participants to the PMIP2 project, the international modeling groups for providing their data for analysis and the Laboratoire des Sciences du Climat et de l'Environnement (LSCE) for collecting and archiving the model data.

5 The PMIP2/MOTIF Data Archive is supported by CEA, CNRS, the EU project MOTIF (EVK2-CT-2002-00153) and the Programme National d'Etude de la Dynamique du Climat (PNEDC). More information is available on <http://pmip2.lsce.ipsl.fr/>. ERA40 reanalysis data are provided by the European Centre for Medium-Range Weather Forecasts, Reading, England, UK (<http://www.ecmwf.int/>). NCEP Reanalysis data provided by the NOAA/OAR/ESRL PSD, Boulder, Colorado, USA, from their Web site at <http://www.cdc.noaa.gov/>.

10

References

- Appenzeller, C., Schwander, J., Sommer, S., and Stocker, T. F.: The North Atlantic Oscillation and its imprint on precipitation and ice accumulation in Greenland, *Geophys. Res. Lett.*, 25, 1939–1942, 1998a. 913, 919, 920
- 15 Appenzeller, C., Stocker, T. F., and Anklin, M.: North Atlantic Oscillation dynamics recorded in Greenland ice cores, *Science*, 282, 446–449, 1998b. 913
- Bahr, A., Arz, H., Lamy, F., and Wefer, G.: Late glacial to Holocene paleoenvironmental evolution of the Black Sea, reconstructed with stable oxygen isotope records obtained on ostracod shells, *Earth Planet. Sci. Lett.*, 241, 863–875, 2006. 919
- 20 Bakke, J., Lie, O., Nesje, A., Dahl, S., and Paasche, O.: Utilizing physical sediment variability in glacier-fed lakes for continuous glacier reconstructions during the Holocene, northern Folgefonna, western Norway, *Holocene*, 15, 161–176, 2005. 919
- Barlow, L. K., White, J. W. C., Barry, R. G., Rogers, J. C., and Grootes, P. M.: The North-Atlantic Oscillation signature in deuterium and deuterium excess signals in the Greenland Ice-Sheet Project 2 ice core, 1840–1970, *Geophys. Res. Lett.*, 20, 2901–2904, 1993. 913
- 25 Braconnot, P., Otto-Bliesner, B., Harrison, S., Joussaume, S., Peterchmitt, J.-Y., Abe-Ouchi, A., Crucifix, M., Driesschaert, E., Fichefet, Th., Hewitt, C. D., Kageyama, M., Kitoh, A., Lan, A., Loutre, M.-F., Marti, O., Merkel, U., Ramstein, G., Valdes, P., Weber, S. L., Yu, Y., and Zhao, Y.: Results of PMIP2 coupled simulations of the Mid-Holocene and Last Glacial Maximum -

Changes in atmospheric variability in a glacial climate

F. S. R. Pausata et al.

Title Page

Abstract

Introduction

Conclusions

References

Tables

Figures



Back

Close

Full Screen / Esc

Printer-friendly Version

Interactive Discussion

Changes in atmospheric variability in a glacial climate

F. S. R. Pausata et al.

Title Page

Abstract

Introduction

Conclusions

References

Tables

Figures

◀

▶

◀

▶

Back

Close

Full Screen / Esc

Printer-friendly Version

Interactive Discussion

Part 1: experiments and large-scale features, *Clim. Past*, 3, 261–277, 2007,

<http://www.clim-past.net/3/261/2007/>. 915

Christoph, M., Ulbrich, U., Oberhuber, J. M., and Roeckner, E.: The role of ocean dynamics for low-frequency fluctuations of the NAO in a coupled ocean-atmosphere GCM, *J. Clim.*, 13, 2536–2549, 2000. 913

Deser, C., Walsh, J. E., and Timlin, M. S.: Arctic sea ice variability in the context of recent atmospheric circulation trends, *J. Clim.*, 13, 617–633, 2000. 919

Donohoe, A. and Battisti, D. S.: Causes of reduced North Atlantic Storm Activity in a CCSM3 simulation of the Last Glacial Maximum, *J. Clim.*, submitted, 2009. 918

Feldstein, S. B.: The recent trend and variance increase of the annular mode, *J. Clim.*, 15, 88–94, 2002. 918

Gladstone, R. et al.: Mid-Holocene NAO: A PMIP2 model intercomparison, *Geophys. Res. Lett.*, 32, L16707, doi:10.1029/2005GL023596, 2005. 913

Glueck, M. F. and Stockton, C. W.: Reconstruction of the North Atlantic oscillation, 1429–1983, *Int. J. Climatol.*, 21, 1453–1465, 2001. 919

Gong, G., Entekhabi, D., and Cohen, J.: A large-ensemble model study of the wintertime AO-NAO and the role of interannual snow perturbations, *J. Clim.*, 15, 3488–3499, 2002. 919

Hurrell, J. W.: Decadal trends in the North Atlantic oscillation – regional temperatures and precipitation, *Science*, 269, 676–679, 1995. 913, 919, 920

Hutterli, M. A., Raible, C. C., and Stocker, T. F.: Reconstructing climate variability from Greenland ice sheet accumulation: An ERA40 study, *Geophys. Res. Lett.*, 32, L23712, doi:10.1029/2005GL024745, 2005. 913, 920

Justino, F. and Peltier, W.: The glacial North Atlantic oscillation, *Geophys. Res. Lett.*, 32, L21803, doi:10.1029/2005GL023822, 2005. 914, 917

Laîné, A., Kageyama, M., Salas-Mèlia, D., Voltaire, A., Rivière, G., Ramstein, G., Planton, S., Tyteca, S., and Petershmitt, J. Y.: Northern hemisphere storm tracks during the last glacial maximum in PMIP2 ocean-atmosphere models, *Clim. Dynam.*, 32, 593–614, 2008. 914

Li, C. and Battisti, D. S.: Reduced Atlantic storminess during last glacial maximum: evidence from a coupled climate model, *J. Clim.*, 21, 3561–3579, 2008. 914, 916, 918

Luo, D., Lupo, A. R., and Wan, H.: Dynamics of eddy-driven low-frequency dipole modes. Part I: A simple model of North Atlantic oscillations, *J. Atmos. Sci.*, 64, 3–28, 2007. 913

Luterbacher, J., Xoplaki, E., Dietrich, D., Rickli, R., Jacobeit, J., Beck, C., Gyalistras, D., Schmutz, C., and Wanner, H.: Reconstruction of sea level pressure fields over the East-

- ern North Atlantic and Europe back to 1500, *Clim. Dynam.*, 18, 545–561, 2002. 913
- Miller, R. L., Schmidt, G. A., and Shindell, D. T.: Forced annular variations in the 20th century intergovernmental panel on climate change fourth assessment report models, *J. Geophys. Res.-Atmos.*, 111, D18101, doi:10.1029/2005JD006323, 2006. 913
- 5 Otto-Bliesner, B. L., Brady, E. C., Clauzet, G., Tomas, R., Levis, S., and Kothavala, Z.: Last glacial maximum and holocene climate in CCSM3, *J. Clim.*, 19, 2526–2544, 2006. 914, 917
- Peltier, W., and Solheim L.: Dynamics of the ice-age Earth: Solid mechanics and fluid mechanics, *J. Phys. IV*, 12, 85–104, 2002. 914, 917
- Peltier, W. R.: Global glacial isostasy and the surface of the ice-age earth: The ice-5G (VM2) model and grace, *Ann. Rev. Earth Planet. Sci.*, 32, 111–149, 2004. 915
- 10 Raible, C., Casty, C. C. et al.: Climate variability-observations, reconstructions, and model simulations for the Atlantic-European and Alpine region from 1500–2100 AD, *Clim. Change*, 79, 9–29, 2006. 913
- Seierstad, I. A. and Bader, J.: Impact of a projected future Arctic Sea Ice reduction on extratropical storminess and the NAO, *Clim. Dynam.*, doi:10.1007/s00382-008-0463-x, in press, 2008. 919
- 15 Shindell, D. T., Miller, R. L., Schmidt, G. A., and Pandolfo, L.: Simulation of recent northern winter climate trends by greenhouse-gas forcing, *Nature*, 399, 452–455, 1999. 913
- Thompson, D. W. J. and Wallace, J. M.: Annular modes in the extratropical circulation. Part I: Month-to-month variability, *J. Clim.*, 13, 1000–1016, 2000. 913
- 20 Voigt, R., Grueger, E., Baier, J., and Meischner, D.: Seasonal variability of Holocene climate: a palaeolimnological study on varved sediments in Lake Jues (Harz Mountains, Germany), *J. Paleolimn.*, 40, 1021–1052, 2008. 919
- Yin, J. H. and Battisti, D. S.: The importance of tropical sea surface temperature patterns in simulations of last glacial maximum climate, *J. Clim.*, 14, 565–581, 2001. 919
- 25

CPD

5, 911–936, 2009

Changes in atmospheric variability in a glacial climate

F. S. R. Pausata et al.

Title Page

Abstract

Introduction

Conclusions

References

Tables

Figures

⏪

⏩

◀

▶

Back

Close

Full Screen / Esc

Printer-friendly Version

Interactive Discussion

Changes in atmospheric variability in a glacial climate

F. S. R. Pausata et al.

Table 1. LGM-PI changes in interannual variability of SLP in the Northern Hemisphere (σ_{NH} of SLP) and in the North Atlantic (σ_{NA} of SLP); fraction of variance explained by the leading EOF (λ_1); amount of raw variability explained by the leading EOF in standard deviation units ($\sqrt{\lambda_1 \sigma_{NA}^2}$); and the amplitude of the seasonal cycle of Northern Hemisphere SLP variability (seasonal cycle of σ_{NH}).

LGM vs. PI	σ_{NH} of SLP	σ_{NA} of SLP	λ_1	$\sqrt{\lambda_1 \sigma_{NA}^2}$	Seasonal cycle of σ_{NH}
CCSM3	–10%	–11%	–34%	–28%	–38%
IPSL	–6%	–6%	–29%	–21%	–30%
HadCM3M2	–16%	–16%	–5%	–18%	–25%
MIROC3.2	+3%	+9%	–16%	0%	–19%

Title Page

Abstract

Introduction

Conclusions

References

Tables

Figures

⏪

⏩

◀

▶

Back

Close

Full Screen / Esc

Printer-friendly Version

Interactive Discussion

Changes in atmospheric variability in a glacial climate

F. S. R. Pausata et al.

Table 2. Pattern correlations for temperature and precipitation anomalies associated with the leading mode of climate variability in CCSM3 and HadCM3M2 simulations.

		Temperature		Precipitation	
		HadCM3M2	CCSM3	HadCM3M2	CCSM3
		PI	LGM	PI	LGM
CCSM3	PI	0.81	0.33	0.70	0.12
HadCM3M2	LGM	0.53	0.41	0.28	0.49

Title Page

Abstract

Introduction

Conclusions

References

Tables

Figures

◀

▶

◀

▶

Back

Close

Full Screen / Esc

Printer-friendly Version

Interactive Discussion



Changes in atmospheric variability in a glacial climate

F. S. R. Pausata et al.

Table 3. Correlations between winter season surface air temperature and PC1 of sea level pressure in the North Atlantic sector for the four locations indicated in Fig. 6.

Winter Season (Temp.)	ERA40	NCEP/NCAR	CCSM3		HADCM3M2	
	1957–2002	1957–2002	PI	LGM	PI	LGM
△ NASA-U (74° N, 50° W)	−0.58	−0.68	−0.39	−0.61	−0.57	0.33
○ Summit (73° N, 37° W)	−0.54	−0.63	−0.15	−0.60	−0.45	−0.08
◇ Labrador (52° N, 60° W)	−0.75	−0.77	−0.46	−0.48	−0.65	−0.55
* Norway (60° N, 6° E)	0.71	0.75	0.61	0.33	0.77	0.70

Title Page

Abstract

Introduction

Conclusions

References

Tables

Figures

⏪

⏩

◀

▶

Back

Close

Full Screen / Esc

Printer-friendly Version

Interactive Discussion

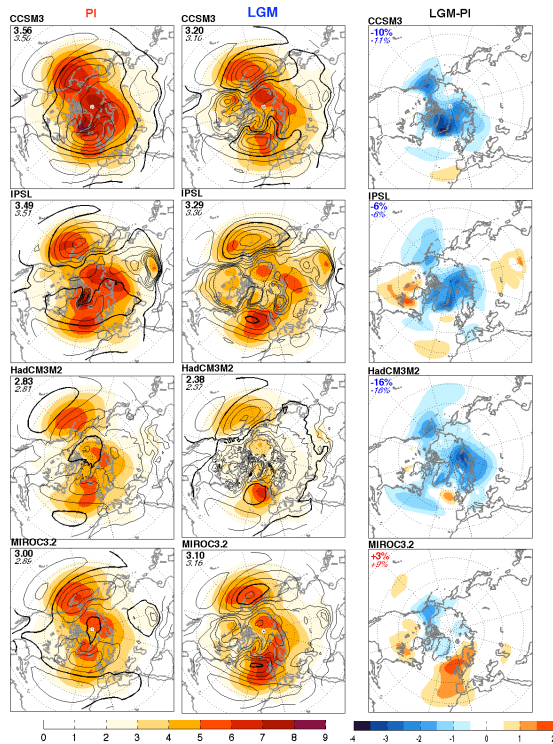


Fig. 1. The mean (contours: 4 hPa interval from 1000 to 1040 hPa; higher values omitted for clarity; bold contour denotes 1016 hPa) and standard deviation (colored shading: hPa) of monthly SLP averaged over all months in simulations of PI (left) and LGM (center) climate. Numbers show the SLP standard deviation area-averaged over the Northern Hemisphere (σ_{NH} in bold) and over the North Atlantic (σ_{NA} in italic). Differences (LGM-PI) are shown in the right panels.

Changes in atmospheric variability in a glacial climate

F. S. R. Pausata et al.

Title Page

Abstract

Introduction

Conclusions

References

Tables

Figures

◀

▶

◀

▶

Back

Close

Full Screen / Esc

Printer-friendly Version

Interactive Discussion

Changes in atmospheric variability in a glacial climate

F. S. R. Pausata et al.

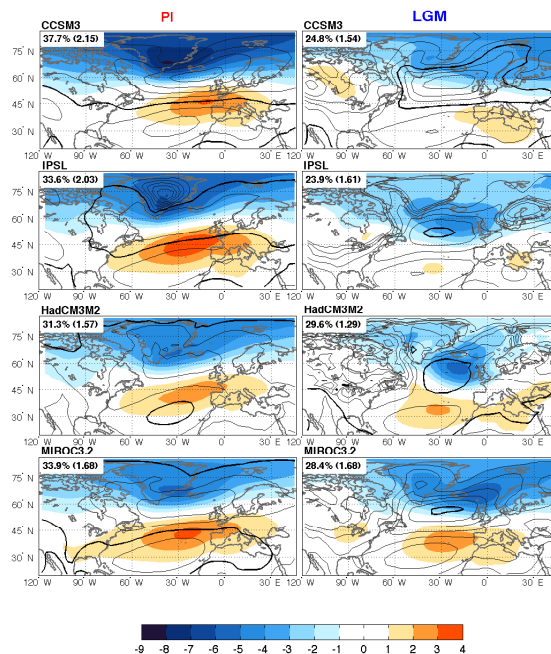


Fig. 2. Leading EOF of monthly SLP anomalies (colored shading: hPa/standard deviation of PC) and SLP climatology (contours: 4 hPa interval from 1000 to 1040 hPa; higher values omitted for clarity; bold contour denotes 1016 hPa) in the North Atlantic sector (all months) for the PI and LGM simulations. Numbers show the amount of variance explained by the first mode both as a percentage of the total variance (λ_1) and as a standard deviation in hPa ($\sqrt{\lambda_1 \sigma_{NA}^2}$).

Title Page

Abstract

Introduction

Conclusions

References

Tables

Figures

◀

▶

◀

▶

Back

Close

Full Screen / Esc

Printer-friendly Version

Interactive Discussion

Changes in atmospheric variability in a glacial climate

F. S. R. Pausata et al.

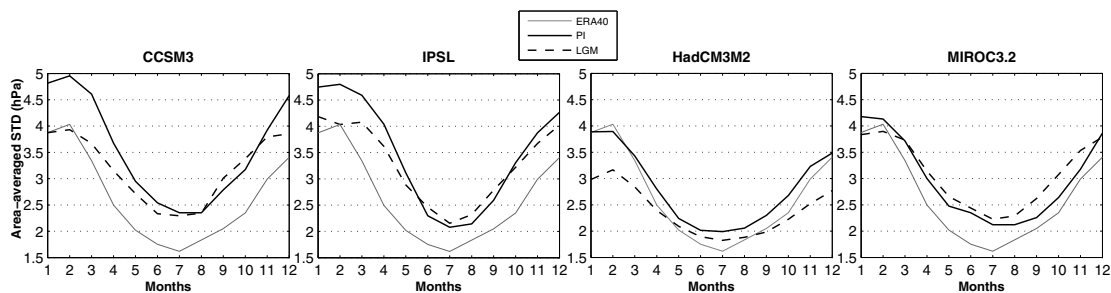


Fig. 3. Seasonal cycle of interannual SLP standard deviation over the Northern Hemisphere in the PI and LGM simulations, and for the ERA40 reanalysis 1957–2002.

Title Page

Abstract

Introduction

Conclusions

References

Tables

Figures

◀

▶

◀

▶

Back

Close

Full Screen / Esc

Printer-friendly Version

Interactive Discussion

Changes in atmospheric variability in a glacial climate

F. S. R. Pausata et al.

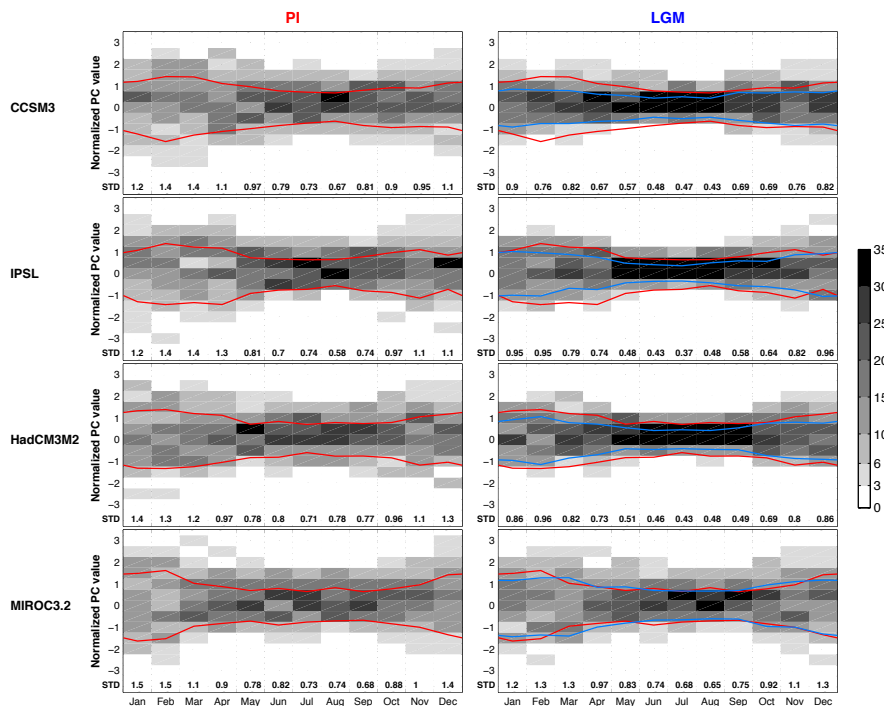


Fig. 4. Histograms of the leading principal component (PC1) of SLP as a function of month. For each month, the PC has been normalized by the standard deviation of the annually averaged PC1 from the PI simulations in each model. This normalization allows for comparison between climate states within a given model. The standard deviations of the PC in these normalized units are indicated along the x -axis for each month and are marked by the lines (red for PI, blue for LGM).

Title Page

Abstract

Introduction

Conclusions

References

Tables

Figures

⏪

⏩

◀

▶

Back

Close

Full Screen / Esc

Printer-friendly Version

Interactive Discussion

Changes in atmospheric variability in a glacial climate

F. S. R. Pausata et al.

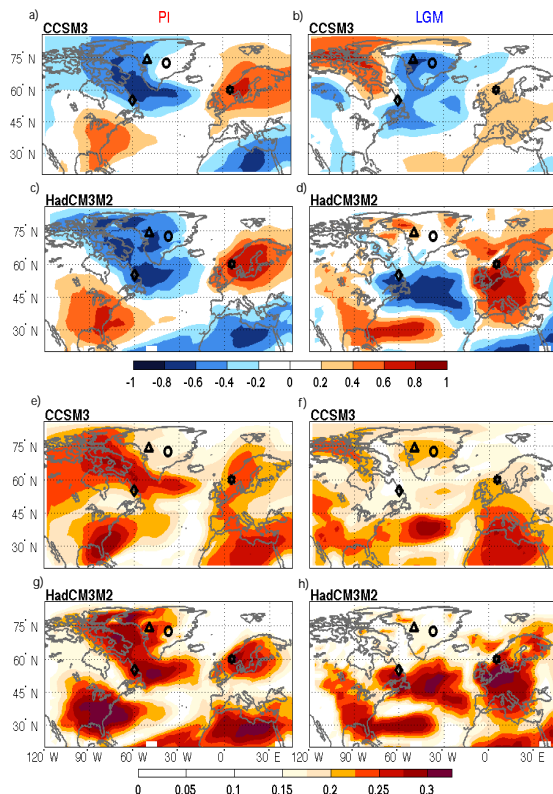


Fig. 5. PI and LGM correlations between North Atlantic winter surface air temperature (November to April) and PC1 (NAO-like index) for CCSM3 (**a**, **b**) and HadCM3M2 (**c**, **d**). An indicator of temperature coherence in the sector for CCSM3 (**e**, **f**) and HadCM3M2 (**g**, **h**): the value at each point is the absolute value of the area-averaged correlation between temperature at that point and the rest of the North Atlantic basin. Markers indicate the locations used in Table 3.

Title Page

Abstract

Introduction

Conclusions

References

Tables

Figures

◀

▶

◀

▶

Back

Close

Full Screen / Esc

Printer-friendly Version

Interactive Discussion

Changes in atmospheric variability in a glacial climate

F. S. R. Pausata et al.

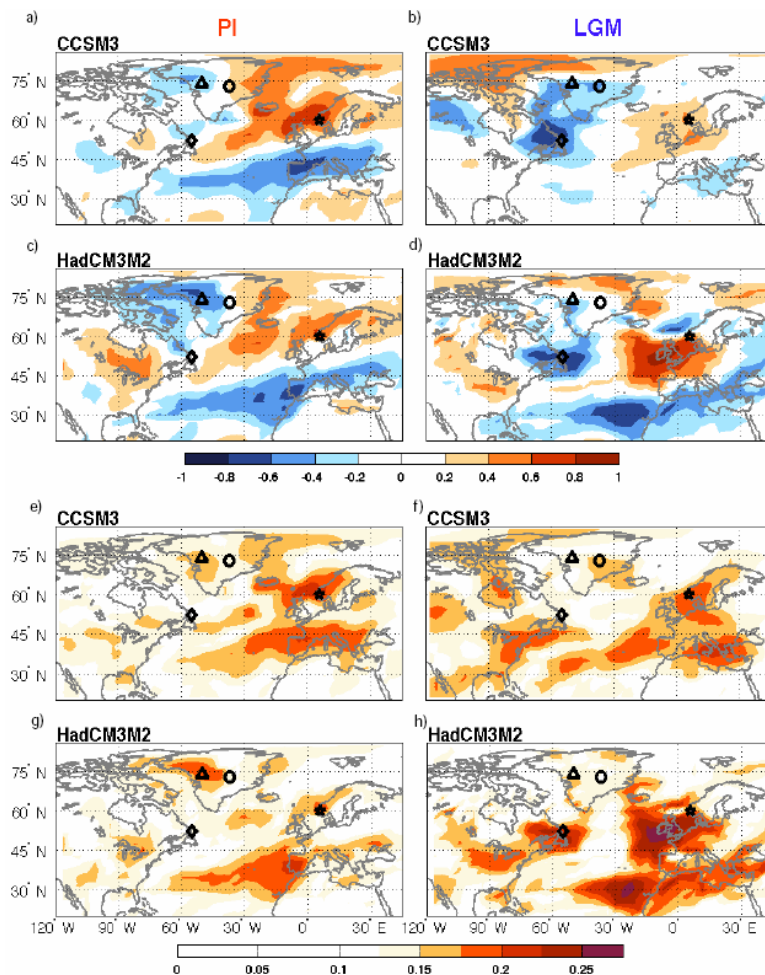


Fig. 6. Same as Fig. 5 for precipitation.

[Title Page](#)[Abstract](#)[Introduction](#)[Conclusions](#)[References](#)[Tables](#)[Figures](#)[◀](#)[▶](#)[◀](#)[▶](#)[Back](#)[Close](#)[Full Screen / Esc](#)[Printer-friendly Version](#)[Interactive Discussion](#)

Changes in atmospheric variability in a glacial climate

F. S. R. Pausata et al.

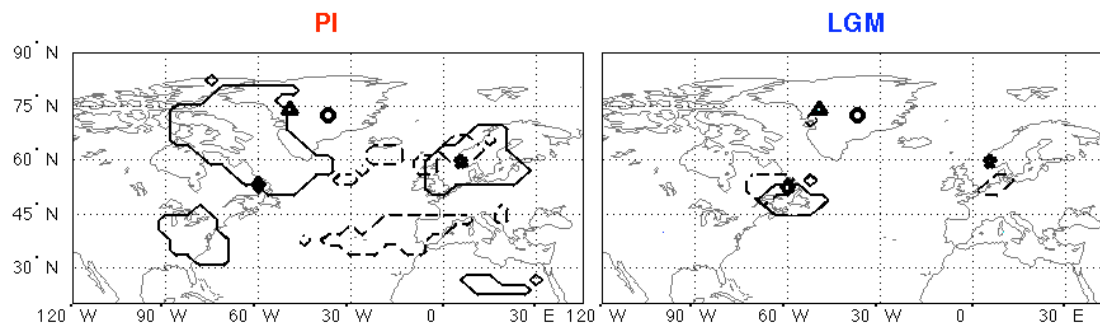


Fig. 7. Solid (dashed) lines represent respectively the areas where the correlation between temperature (precipitation) and the PC1 of the SLP for all the models is greater than 0.4 in absolute value in the PI and LGM simulations.

Title Page

Abstract

Introduction

Conclusions

References

Tables

Figures

◀

▶

◀

▶

Back

Close

Full Screen / Esc

Printer-friendly Version

Interactive Discussion

Changes in atmospheric variability in a glacial climate

F. S. R. Pausata et al.

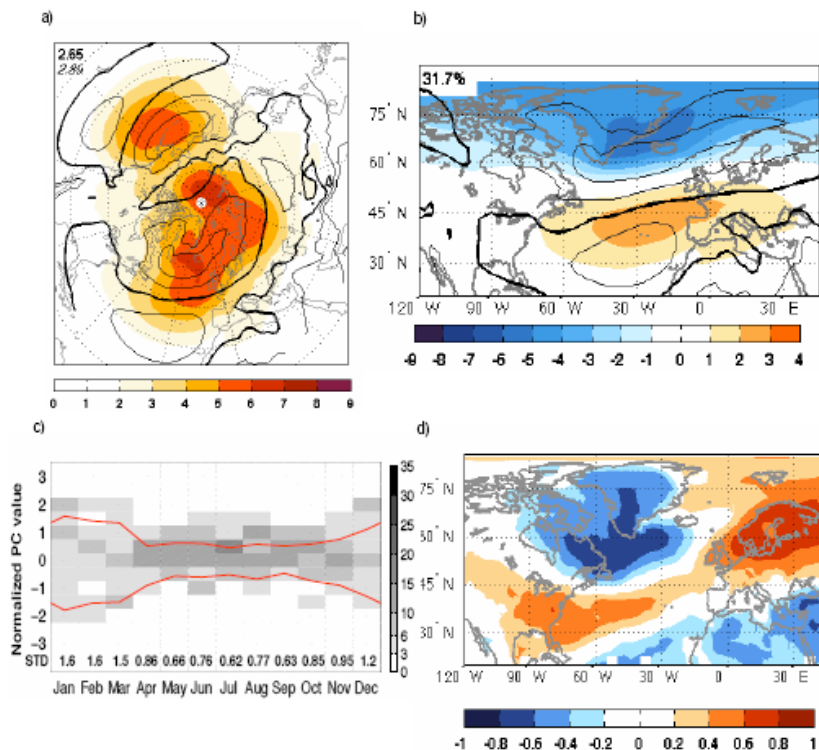


Fig. 8. ERA40 reanalysis for the period 1957–2002; **(a)** The mean (contours) and standard deviation (colored shading: hPa) of monthly SLP averaged over all months; **(b)** Leading EOF of monthly SLP anomalies (colored shading: hPa/standard deviation of PC) and SLP climatology (contours) in the North Atlantic sector (all months). Numbers show the amount of variance explained by the first mode both as a percentage of the total variance (λ_1); in both panels the contours have 4 hPa interval from 1000 to 1040 hPa, bold contour denotes 1016 hPa; **(c)** Histograms of the leading principal component (PC1) of SLP as a function of month. For each month, the PC has been normalized by the standard deviation of the annually averaged PC1. The standard deviations of the PC in these normalized units are indicated along the x-axis for each month and are marked by the lines; **(d)** Correlations between North Atlantic winter surface air temperature and PC1.

Title Page

Abstract

Introduction

Conclusions

References

Tables

Figures

◀

▶

◀

▶

Back

Close

Full Screen / Esc

Printer-friendly Version

Interactive Discussion